

# Particle-in-cell plasma simulation with OmpSs-2

Rodrigo Arias Mallo

June 16, 2019



# Contents

<b>1</b>	<b>Introduction</b>	<b>5</b>
1.1	Motivation . . . . .	5
1.2	Objectives . . . . .	5
1.3	Context . . . . .	5
1.4	Structure . . . . .	5
<b>2</b>	<b>Related work</b>	<b>7</b>
<b>I</b>	<b>Theory</b>	<b>9</b>
<b>3</b>	<b>Plasma introduction</b>	<b>11</b>
<b>4</b>	<b>Plasma simulation</b>	<b>13</b>
4.1	The particle-in-cell method . . . . .	13
4.2	Particle mover . . . . .	13
4.2.1	Boris integrator . . . . .	13
4.3	Charge accumulation . . . . .	14
4.4	Field equations . . . . .	14
<b>5</b>	<b>Discrete model</b>	<b>15</b>
5.1	Charge assignment . . . . .	15
5.2	Field equations . . . . .	16
5.2.1	Electric potential . . . . .	16
5.2.2	LU decomposition . . . . .	16
5.2.3	Multiple Fourier Transform (MFT) . . . . .	17
5.2.4	Electric field . . . . .	18
5.3	Force interpolation . . . . .	18
5.4	Equations of motion . . . . .	19
5.4.1	Boris integrator . . . . .	19
<b>II</b>	<b>Computation</b>	<b>21</b>
<b>6</b>	<b>Sequential simulator</b>	<b>23</b>
6.1	Design . . . . .	23
6.2	Validation . . . . .	23

6.2.1	Two particle test . . . . .	24
6.2.2	Two stream instability . . . . .	24
6.2.3	Cyclotron frequency . . . . .	24
<b>7</b>	<b>Parallelization techniques</b>	<b>27</b>
7.1	Message Passing Interface . . . . .	27
7.1.1	Concepts . . . . .	27
7.1.2	Implementations . . . . .	28
7.2	OmpSs-2 . . . . .	28
7.2.1	Concepts . . . . .	28
<b>8</b>	<b>Simulator design</b>	<b>29</b>
8.1	Field solver . . . . .	29
<b>9</b>	<b>The simulator</b>	<b>31</b>
9.1	Data structures . . . . .	31
9.2	Simulation flow . . . . .	31
9.2.1	Initialization . . . . .	32
9.2.2	Loop . . . . .	33
9.2.3	Finish . . . . .	33
<b>10</b>	<b>Communication</b>	<b>35</b>
10.1	Particle communication . . . . .	35
10.1.1	Exchange in X . . . . .	35
10.1.2	Exchange in Y . . . . .	37
<b>11</b>	<b>Analysis</b>	<b>41</b>
11.1	Analysis with varying inputs . . . . .	42
<b>12</b>	<b>Configuration</b>	<b>43</b>
<b>13</b>	<b>Caveats and limitations</b>	<b>45</b>

# Chapter 1

## Introduction

It may be surprising to find out that the most common state of matter is plasma when we look at the universe. A plasma is an ionized gas consisting of ions and free electrons distributed over a region in space. in which at least one electron of the atom is separated, so it remains positively charged (ionized) [1]. Usually this happens in the vacuum

### 1.1 Motivation

### 1.2 Objectives

### 1.3 Context

### 1.4 Structure

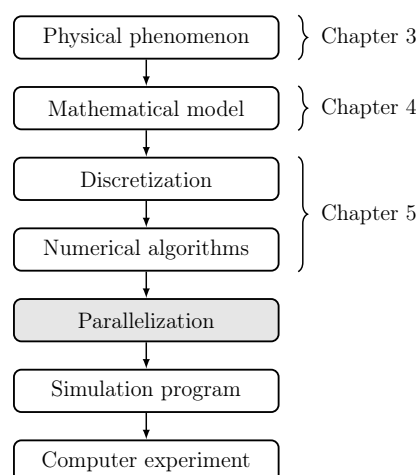


Figure 1.1: Principal steps in computer experiment

The structure of the document follows the diagram shown in the figure 1.1. In chapter 1, plasma is described as a physical phenomenon and we focus on the

relevant properties that we want to study, from which we derive a mathematical model. In chapter 4. The discretization of the mathematical model allows the computer simulation by using numerical algorithms.

# Chapter 2

## Related work

[Briefly talk about other simulation software and techniques. Also we may want to add some historical references.]





# Part I

## Theory



# Chapter 3

## Plasma introduction

*Talk about what is a plasma, and why is of interest*



# Chapter 4

## Plasma simulation

### 4.1 The particle-in-cell method

Solving the Vlasov equation requires a large amount of numerical resources. The particle in cell method, approximates the solution by discretization of the fields.

The method is divided in four main phases:

- Particle motion.
- Charge accumulation.
- Solve field equation.
- Interpolation of fields in particle position.

### 4.2 Particle mover

In order to move the particles, the equations of motion need to be solved:

$$m \frac{d\mathbf{v}}{dt} = q(\mathbf{E} + \mathbf{v} \times \mathbf{B}) \quad (4.1)$$

$$\frac{d\mathbf{v}}{dt} = \mathbf{v} \quad (4.2)$$

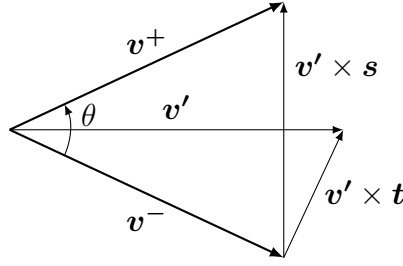
Several methods are available, but we will focus on the Boris integrator.

#### 4.2.1 Boris integrator

Consists of three steps:

1. Add half of the electric impulse
2. Rotate
3. Add the remaining half electric impulse

The Boris integrator computes the velocity of a particle in a constant electric field  $\mathbf{E}$  and a constant magnetic field  $\mathbf{B}$ . We have the velocity  $\mathbf{v}_{t-\Delta t/2}$  of the particle at  $t - \Delta t/2$  as we use the leapfrog integrator.

Figure 4.1: Velocity space rotation from  $\mathbf{v}-$  to  $\mathbf{v}+$ 

**Add half electric impulse** We define  $\mathbf{v}^-$  as the velocity after half a electric impulse:

$$\mathbf{v}^- = \mathbf{v}_{t-\Delta t/2} + \frac{q\mathbf{E}}{m} \frac{\Delta t}{2}$$

**Rotate for the magnetic field** The rotation is done in two steps, first the half rotation is computed, with an angle of  $\theta/2$ :

$$\mathbf{v}' = \mathbf{v}^- + \mathbf{v}^- \times \mathbf{t}$$

Then the rotation is completed by symmetry, using the  $\mathbf{s}$  vector

$$\mathbf{s} = \frac{2\mathbf{t}}{1 + \mathbf{t}^2}$$

as

$$\mathbf{v}^+ = \mathbf{v}^- + \mathbf{v}' \times \mathbf{s}$$

### 4.3 Charge accumulation

The charge density  $\rho$  is a scalar field

### 4.4 Field equations

Once we have the charge density  $\rho$  we can compute the electric field  $\mathbf{E}$  by the integration of the field equations

$$\mathbf{E} = -\nabla\phi \tag{4.3}$$

$$\nabla \cdot \mathbf{E} = \frac{\rho}{\epsilon_0} \tag{4.4}$$

Which can be combined into the Poisson equation

$$\nabla^2\phi = -\frac{\rho}{\epsilon_0} \tag{4.5}$$

Different methods can be used to obtain the electric field, but we will focus on matrix and spectral methods.

# Chapter 5

## Discrete model

The mathematical model is discretized in algebraic operations, in order to be computable.

### 5.1 Charge assignment

At each grid point  $g$  at  $\mathbf{x}$  we accumulate the charge of each particle  $p$  in  $\mathbf{x}_p$  as

$$\rho(\mathbf{x}) = \sum_p q W(\mathbf{x} - \mathbf{x}_p) + \rho_0 \quad (5.1)$$

The background charge density  $\rho_0$  is used to neutralize the total charge when is non-zero. The weighting function  $W$  determines the shape of the particle charge. Different schemes can be used to approximate the charge density from the particles. We will focus on bilinear interpolation for it's simplicity and low computation requirements. The corresponding weighting function can be written as

$$W(\mathbf{x}) = \begin{cases} \left(1 - \frac{|x|}{\Delta x}\right) \left(1 - \frac{|y|}{\Delta y}\right) & \text{if } -\Delta \mathbf{x} < \mathbf{x} < \Delta \mathbf{x} \\ 0 & \text{otherwise} \end{cases} \quad (5.2)$$

Notice that a particle  $p$  always affects the four enclosing grid points in the neighbourhood  $\mathcal{N}(p)$ , but more complex interpolation methods may extend the update region even further. It may be noted that the increase in smoothing, at computation expense, can gain from the reduced number of particles needed to obtain a similar result, avoiding nonphysical effects. The particle  $p$  has a uniform charge area, centered at the particle position  $\mathbf{x}_p$ , with size  $\Delta \mathbf{x}$ , as shown in the figure 5.1. Each grid point  $A, B, C$  and  $D$  receives the amount of charge weighed by the area  $a, b, c$  and  $d$ . It can be observed that the area is equal to the opposite region, when the particle  $p$  is used to divide the grid cell. The particle shape can be altered later in the Fourier space, without large computation effort, in case the solver already computes the FFT.

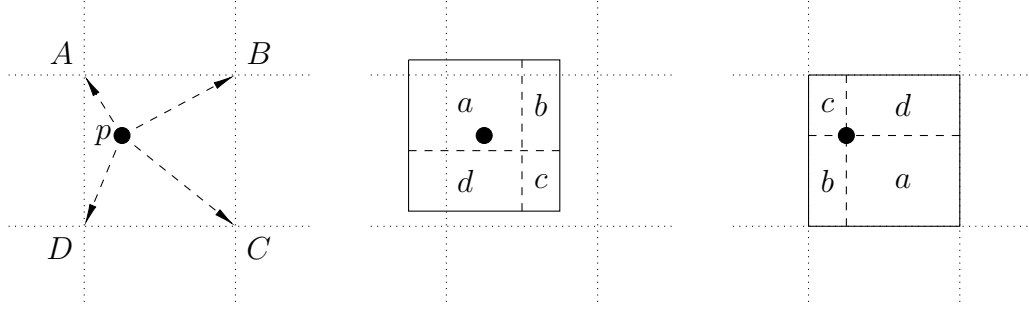


Figure 5.1: Interpolation of particle  $p$  charge into the four grid points A to D.

## 5.2 Field equations

In order to compute the electric field  $\mathbf{E}$ , the electric potential  $\phi$  is generally needed, which can be obtained from the charge density  $\rho$ .

### 5.2.1 Electric potential

Several methods are available to solve the Poisson equation (Eq. 4.5).

**Iterative methods** such as Jacobi, Gauss-Seidel, Successive Over Relaxation (SOR), Chebyshev acceleration are some of the most familiar methods to solve the Poisson equation.

**Matrix methods** The equations from finite differencing the mesh are considered a large system of equations. We can find in this methods the Thomas Tridiagonal algorithm, Conjugate-Gradient, LU or Incomplete Decomposition.

**Spectral methods** Also known as Rapid Elliptic Solvers (RES) are a family of methods that use the fast Fourier transform (FFT). Are know for being usually faster than the previous ones, with a complexity in  $O(N_g \log_2 N_g)$

We will only focus on the LU for small problems and for testing, and spectral methods, more specific on the Multiple Fourier Transform (MTF) method, as it is the main method implemented in the simulator, due to its relative simplicity and low computational complexity.

### 5.2.2 LU decomposition

For two dimensions, we can approximate the solution using the second order centered finite differences (with an error proportional to  $\Delta x^2 \Delta y^2$ ), as

$$\frac{\phi(x-1, y) + \phi(x, y-1) - 4\phi(x, y) + \phi(x+1, y) + \phi(x, y+1)}{\Delta x^2 \Delta y^2} = -\frac{\rho(x, y)}{\epsilon_0} \quad (5.3)$$

which leads to a system of  $N_g$  linear equations and can be also written in matrix form

$$A\phi = -\frac{\Delta x^2 \Delta y^2 \rho}{\epsilon_0} \quad (5.4)$$



The  $N_g \times N_g$  coefficient matrix  $A$  has non-zero coefficients only at  $a_{ii} = 4$  and  $a_{ij} = -1$  with  $j \in \{i+1, i-1, i+N_x, i-N_x\} \bmod N_x$ , for all  $0 \leq i \leq N_g$ . However, the matrix  $A$  is singular, so the system of equations has infinite solutions. Boundary conditions can be added to get a unique solution. The extra equation  $\phi(0,0) = 0$  leads to a system with only one solution, but with one extra equation. In order to keep the matrix  $A$  square, the following steps may be taken:

1. Subtract the extra equation  $\phi(0,0) = 0$  to the first row of  $A$ , with the only change in the coefficient to  $a_{11} = 3$ .
2. Add all first  $N_g$  equations: Each equation has one coefficient of 4 and four of  $-1$  except the first equation. Also we assume the total charge density is zero, obtaining  $\phi(0,0) = 0$ .
3. Subtract it from the last equation, which leads to a zero coefficient that can be removed.

The only change that remains is at the coefficient  $a_{11} = 3$ . Now the matrix  $A$  is squared and non-singular and has only one solution and can now be solved with the  $LU$  method.

The  $LU$  decomposition, with a complexity in  $O(2/3N_g^3)$ , can be used to form two systems of equations that can be solved faster. If we rewrite the system of equations 5.4 as the usual form  $Ax = b$  with

$$x = \phi, \quad b = -\frac{\Delta x^2 \Delta y^2 \rho}{\epsilon_0} \quad (5.5)$$

Then we can use the decomposition  $A = LU$  to form two systems of equations

$$Ux = y, \quad Ly = b \quad (5.6)$$

which can be solved in complexity  $O(2N_g^2)$ .

### 5.2.3 Multiple Fourier Transform (MFT)

The general second-order PDE with constant coefficients and periodic boundary conditions

$$a \frac{\partial^2 \phi}{\partial x^2} + b \frac{\partial \phi}{\partial x} + c\phi + d \frac{\partial^2 \phi}{\partial y^2} + e \frac{\partial \phi}{\partial y} + f\phi = g(x, y) \quad (5.7)$$

can be solved by using the FFT. If we expand  $\phi$  and  $g$  in a finite double Fourier series, we obtain

$$\phi(x, y) = \sum_{k,l} \hat{\phi}(k, l) \exp\left(\frac{2\pi i(xk + yl)}{n}\right) \quad (5.8)$$

and

$$g(x, y) = \sum_{k,l} \hat{g}(k, l) \exp\left(\frac{2\pi i(xk + yl)}{n}\right) \quad (5.9)$$

which now can be substituted in the Eq. 5.7, to obtain

$$\hat{\phi}(k, l) = \hat{G}(k, l) \hat{g}(k, l), \quad 0 < k < N_x, 0 < l < N_y \quad (5.10)$$

with for a unit mesh

$$\hat{G}(k, l) = \left[ 2a \left( \cos \frac{2\pi k}{n} - 1 \right) + ib \sin \frac{2\pi k}{n} + c + \right. \\ \left. 2d \left( \cos \frac{2\pi l}{n} - 1 \right) + ie \sin \frac{2\pi l}{n} + f \right]^{-1} \quad (5.11)$$

To solve the Poisson equation, discretized as Eq. 5.3, we have  $a = d = 1$  and  $b = c = e = f = 0$  so we can simplify  $\hat{G}(k, l)$  as

$$\hat{G}(k, l) = \frac{1}{2} \left[ \cos \frac{2\pi k}{n} + \cos \frac{2\pi l}{n} - 2 \right]^{-1} \quad (5.12)$$

Let  $g = -\Delta x^2 \Delta y^2 \rho / \epsilon_0$ , then the steps to compute the electric potential can be summarized as follows:

$$g \xrightarrow{\text{FFT}} \hat{g} \xrightarrow{\hat{G}} \hat{\phi} \xrightarrow{\text{IFFT}} \phi$$

1. Compute the complex FFT  $\hat{g}$  of  $g$
2. Multiply each element of  $\hat{g}$  by the corresponding complex coefficient  $\hat{G}$ , to obtain  $\hat{\phi}$
3. Compute the inverse FFT of  $\hat{\phi}$  to get  $\phi$

The complexity in the worst case is in  $O(N_g \log_2 N_g)$  with the number of total points in the grid  $N_g$ .

### 5.2.4 Electric field

The electric field  $\mathbf{E}$  can then be obtained by centered first order finite differences in each dimension

$$\mathbf{E}_x(x, y) = \frac{\phi(x-1, y) - \phi(x+1, y)}{2 \Delta x} \\ \mathbf{E}_y(x, y) = \frac{\phi(x, y-1) - \phi(x, y+1)}{2 \Delta y} \quad (5.13)$$

## 5.3 Force interpolation

The force acting on a particle  $p$  can be decomposed in two main parts, the electric and magnetic force  $\mathbf{F} = \mathbf{F}_E + \mathbf{F}_B$ .

The electric force  $\mathbf{F}_E$  is computed similarly as the charge deposition, but in the reverse order. The force  $\mathbf{F}_E$  is interpolated from the electric field  $\mathbf{E}$  of the neighbour grid points  $\mathcal{N}(p)$ , using the same interpolation function  $W$ .

$$\mathbf{F}_E = q \sum_{g \in \mathcal{N}(p)} W(\mathbf{x}_p - \mathbf{x}_g) \mathbf{E}(\mathbf{x}_g) \quad (5.14)$$

Notice that a particle  $p$  only needs the values of the electric field in the neighbourhood  $\mathcal{N}(p)$ .

The magnetic force  $\mathbf{F}_B$  is constant in the simulator, as we only consider a fixed background magnetic field  $\mathbf{B}_0$ . For a particle  $p$  with velocity  $\mathbf{v}$  can be written as

$$\mathbf{F}_B = q(\mathbf{v} \times \mathbf{B}_0) \quad (5.15)$$

## 5.4 Equations of motion

In order to move the particles, the equations of motion need to be solved:

$$\frac{d\mathbf{x}}{dt} = \mathbf{v} \quad (5.16)$$

$$m \frac{d\mathbf{v}}{dt} = \mathbf{F} \quad (5.17)$$

The *leap-frog* method is a common integration scheme with second-order accuracy and an error proportional to  $\Delta t^2$ . The name describes the behavior of the position and velocity, which are updated at interleaved time steps, similarly to the trajectory of a frog. The method is time reversible with a stability far superior of other higher-order integration methods, such as fourth order Runge-Kutta. A more in depth stability analysis can be found in Chapter 4 of Hockney and Eastwood book [3]. The discretized equations can be written as

$$\frac{\mathbf{x}^{n+1} - \mathbf{x}^n}{\Delta x} = \mathbf{v}^{n+1/2} \quad (5.18)$$

$$m \frac{\mathbf{v}^{n+1/2} - \mathbf{v}^{n-1/2}}{\Delta x} = \mathbf{F}(\mathbf{x}^n) \quad (5.19)$$

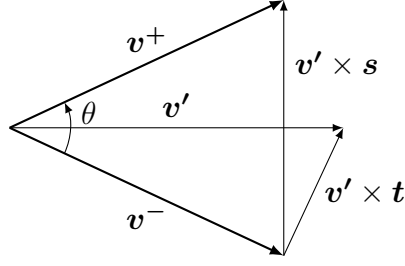
Several methods are available, but we will focus on the Boris integrator.

### 5.4.1 Boris integrator

Consists of three steps:

1. Add half of the electric impulse
2. Rotate
3. Add the remaining half electric impulse

The Boris integrator computes the velocity of a particle in a constant electric field  $\mathbf{E}$  and a constant magnetic field  $\mathbf{B}$ . We have the velocity  $\mathbf{v}_{t-\Delta t/2}$  of the particle at  $t - \Delta t/2$  as we use the leapfrog integrator.

Figure 5.2: Velocity space rotation from  $\mathbf{v}-$  to  $\mathbf{v}+$ 

**Add half electric impulse** We define  $\mathbf{v}^-$  as the velocity after half a electric impulse:

$$\mathbf{v}^- = \mathbf{v}_{t-\Delta t/2} + \frac{q\mathbf{E}}{m} \frac{\Delta t}{2}$$

**Rotate for the magnetic field** The rotation is done in two steps, first the half rotation is computed, with an angle of  $\theta/2$ :

$$\mathbf{v}' = \mathbf{v}^- + \mathbf{v}^- \times \mathbf{t}$$

Then the rotation is completed by symmetry, using the  $\mathbf{s}$  vector

$$\mathbf{s} = \frac{2\mathbf{t}}{1 + \mathbf{t}^2}$$

as

$$\mathbf{v}^+ = \mathbf{v}^- + \mathbf{v}' \times \mathbf{s}$$

# Part II

## Computation



# Chapter 6

## Sequential simulator

In order to begin the implementation of the simulator, an initial version was considered with the minimum complexity, to verify the correctness of the model. A graphic subsystem was built with MathGL and OpenGL to produce realtime plots of different elements of the simulation. Of special interest are the particle motion, the electric potential and the electric field.

The language of choice was C for the low overhead, the lack of automatic memory management, the support of different libraries planned in future versions and the low level design, which allowed us to define most of the data structures close to the byte level.

### 6.1 Design

The simulator initially only supported one group of particles of the same charge and mass, denominated specie. Each particle was implemented as a structure with a given index  $i$ , a position vector  $\mathbf{x}$ , velocity  $\mathbf{v}$  and other extra fields such as the interpolated electric field at the particle position  $\mathbf{E}$ . Only one dimension was implemented for the first tests, but soon extended to two dimensions. The fields were allocated in contiguous arrays, with the  $x$  dimension aligned with the cache line, also called row-major storage.

The configuration of the simulation is specified in plain configuration files, with the syntax defined by the `libconfig` library. Is important to allow the user to specify comments in the configuration files, as well as scientific notation in different values. Additionally, the specification of multiple species benefits from the sub-configuration block feature, which leads to a more intuitive representation. The detailed configuration is described in the chapter 12.

The solver used was initially the *LU* decomposition, used from the *GSL* numeric library [2], as the only focus was to obtain valid results, ignoring the performance. All implementations are tested beforehand with some test cases designed in `octave`.

### 6.2 Validation

A set of different tests were designed to determine the correctness of the simulation.

### 6.2.1 Two particle test

A simple one-dimensional test consists of two electrons placed at some distance different of  $L/2$  with no initial speed. The analytical solution is known and the motion should follow a harmonic oscillation trajectory. The energy conservation can be observed in the figure 6.1, where the total energy only varies due to the interpolation noise as the time  $t$  grows in the  $x$  axis.

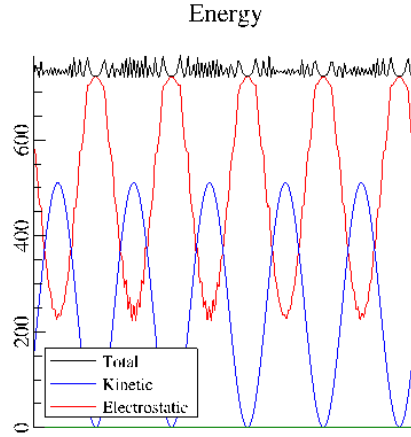


Figure 6.1: Energy conservation in two particle test

### 6.2.2 Two stream instability

Another example in one dimension is the two stream instability, which consists of two streams of particles with opposite velocity. With 500 particles in each stream, a very characteristic set of vortices are created in the position-velocity phase space, which can be shown in the figure 6.2.

### 6.2.3 Cyclotron frequency

In a simulation with two dimensions and a fixed background magnetic field  $\mathbf{B}_0$ , a charged particle with some initial velocity should describe a circular orbit. The radius  $r_g$  known as the Larmor or gyroradius, can be computed analytically as

$$r_g = \frac{mv}{|q|B} \quad (6.1)$$



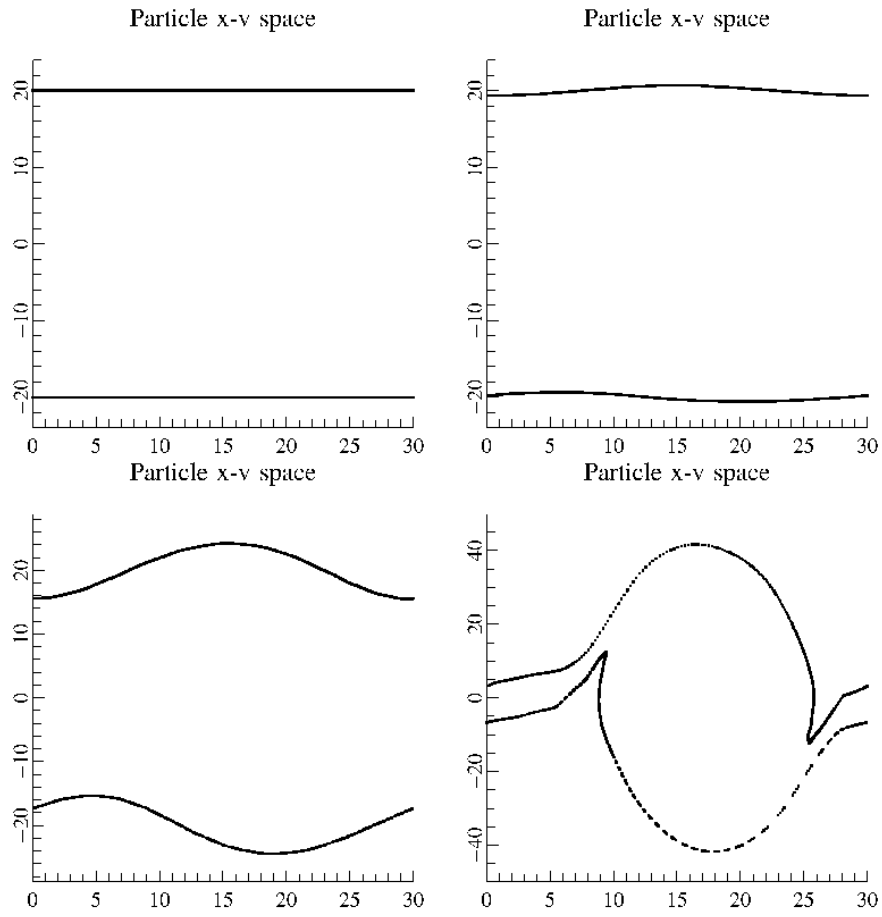


Figure 6.2: Phase space position-velocity of the two stream instability, shown at iterations: 0, 200, 400 and 600 (left to right, top to bottom)



# Chapter 7

## Parallelization techniques

### 7.1 Message Passing Interface

From the need of standarize communications in a distributed computing environment, the first draft was proposed in 1992 at the Workshop on Standards for Message Passing in a Distributed Memory Environment, and has now become one of the most used communication protocol in HPC. The Message Passing Interface (MPI) provides a simple to use set of routines to allow processes distributed among different nodes to communicate efficiently.

#### 7.1.1 Concepts

**Communicator** A communicator refers to a group of processes, in which each has assigned a unique identifier called the *rank*.

**Point-to-point communication** In order for a process to exchange information with another process, the MPI standard defines what are called point-to-point communication routines. The most common examples are `MPI_Send` to send data, and `MPI_Recv` for the reception. Both routines need the process rank of the process to stablish the connection. Additionally a tag is used to label each message, which can be specified in the reception to filter other messages.

**Blocking communication** The standard defines various types of communication methods for sending and receiving data. The so called blocking routines are designed such that the call does not return until the communication has been done. In the `MPI_Send` case, the call returns when the sending data can be safely modified, as has been sent or buffered. In the case of `MPI_Recv` the routine only returns when the data has been received.

**Non-blocking communication** Similarly as with the blocking communication, the routines `MPI_Isend` and `MPI_Irecv` don't wait until the message is sent or received to return. They return immediately, and the communication status can be checked with `MPI_Test` or the process can wait until the communication request has finished with `MPI_Wait`.

### 7.1.2 Implementations

## 7.2 OmpSs-2

OmpSs-2 is the next generation of the OmpSs programming model, composed of a set of directives and library routines. Mixes from OpenMP the annotation of source code to parallelize some sections with the StarSs execution model, based on a thread-pool design pattern.

### 7.2.1 Concepts

**Task** In OmpSs-2 a task is a section of code that can be executed independently by the runtime schedule. A task may have associated dependencies which lets the scheduler determine in wich order is allowed to execute the tasks. An example annotation of a task:

**Parallelization** Unless there is a unmet dependency, all tasks ready to run are executed in parallel, up to the number of CPU cores available to the runtime.

**Task synchronization** It may be possible that at some point in the execution all pending task are required to finish in order to continue. The directive `taskwait` allows the programmer to specify that the runtime must wait for completion of all previous created tasks.

# Chapter 8

## Simulator design

[After determining the mathematical model and the discretization, we want to begin the discussion on how to build the simulator.]

### 8.1 Field solver

Talk about MFT and the data layout.



# Chapter 9

## The simulator

[This chapter is focused on the simulator implementation]

### 9.1 Data structures

The simulator is designed for space domains of one or two dimensions. In order to parallelize the computation of each step, the space domain is distributed in blocks. First the space domain is split in one specific dimension into MPI blocks, which will be distributed among each compute node. Communications will be needed to share information between MPI blocks.

The second hierarchy splits MPI blocks into task blocks, which can run in parallel inside a compute node. Communications are not needed, as we can use shared memory in the same compute node.

Inside each task block, we have a small portion of the space domain: the grid points of the fields and the particles inside the physical space of the block. Additionally, ghost points are placed at the boundaries of the positive neighbours in each dimension of the problem.

A summary of the data layout can be seen in the figure 9.1, where the physical placement of each block corresponds to the physical position of the grid points. The 1D domain has 2 MPI blocks with 3 task blocks each, and 3 grid points per block with 1 ghost point. In total, the space is discretized in 18 grid points, which require 24 with the ghost points.

Similarly, for 2D the number of ghost points increase, as the frontier now has 2 dimensions, leading to blocks with 6 grid points and 6 ghost points. The whole domain is discretized in 120 grid points, a total of 240 with ghost points.

### 9.2 Simulation flow

The simulation follows a very precise set of steps to ensure the correct behavior of the physical simulation. Three main stages can be easily identified: Initialization, loop and finish.

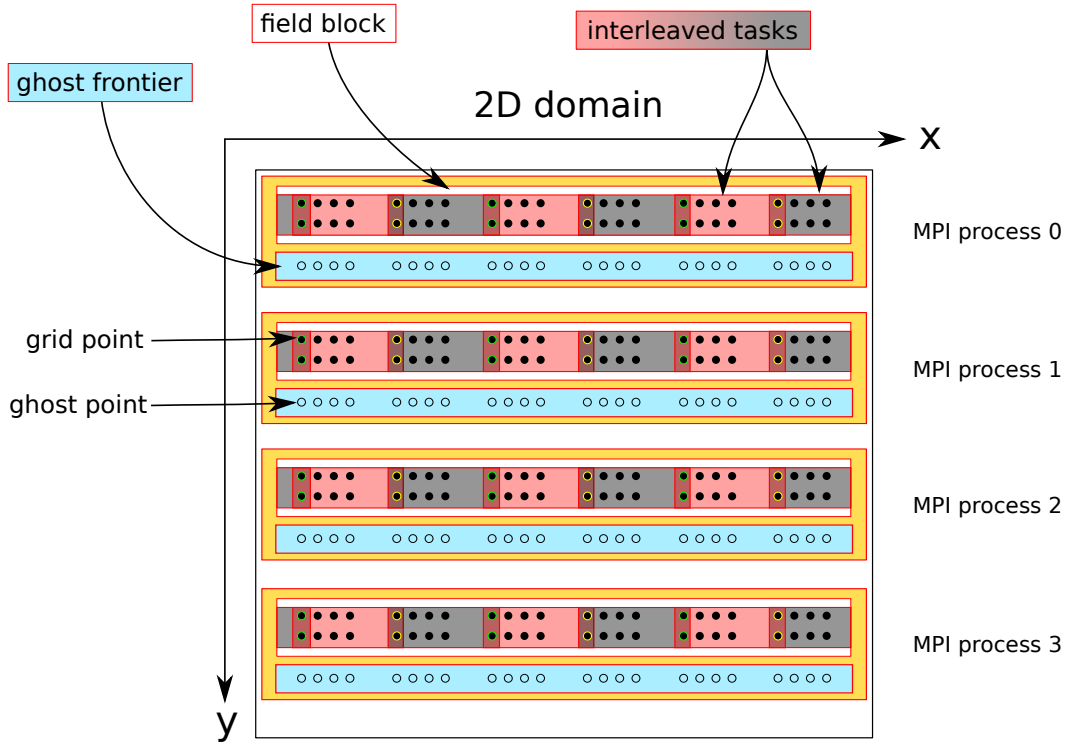


Figure 9.1: Domain blocks

### 9.2.1 Initialization

The iteration counter is initially set to  $-2$ , as we are going to do two previous phases before the simulation begins:

**Allocation phase** After  $P$  processes were created (as in MPI processes), now we create the different structures to hold the simulation data. First the fields are distributed into task blocks, grouped in each process. For each specie, we distribute the particles based on the particle index  $p_i$ , minimizing the difference of the number of particles between blocks. The position, velocity and other parameters are set on each particle, independently of the actual block they reside.

Once all particles are initialized, we begin to move them to the correct block, based on the particle position, and increment the iteration counter. Finally, the charge density field  $\rho$  is initially computed, as we want the begin the simulation with the computation of the electric field  $E$  from  $\rho$

**Rewind phase** The simulation time is not advanced equally for the speed and position of the particles. At time  $t$  the velocity computed at time  $t + \Delta t/2$  whereas the position is computed at time  $t$ . In order to begin the simulation, the velocity of the particles is advanced half time-step backwards in time. This extra step is computed at the iteration  $i = -1$ , as we need the iteration counter to be always increasing (as is used in the message exchange as unique identifier).



### 9.2.2 Loop

The loop of the simulation perform four main phases:

- Solve field equation to get  $E$  from  $\rho$ .
- Interpolate  $E$  at particle positions  $E_p$ .
- Particle motion based on  $E_p$  and  $B_0$ .
- Accumulate charge density  $\rho$  at the new position of particles.

#### Solver

We use the MFT method to solve the equation:

$$\nabla^2 E = -\frac{\rho}{\epsilon_0} \tag{9.1}$$

### 9.2.3 Finish

Here we hopefully save some information of the simulation to disk...



# Chapter 10

## Communication

Different communications are detailed in this chapter, such as particle and frontier communications.

### 10.1 Particle communication

When the particles are moved, due to the interaction with the electric field and the magnetic field, their position can exceed the boundaries of the chunk where they reside. After updating the position of each particle, the ones that exceed the chunk must be translated to the correct one. The process of particle communication is done in two stages: first the particles are moved in the X dimension, then in the Y. Several steps are required in each stage.

#### 10.1.1 Exchange in X

All chunks in the X dimension reside in one MPI process, so the exchange of particles can be done by shared memory. Care must be taken to avoid concurrent writes in the same chunk by different tasks. The proposed solution avoids the problem by using temporal queues in each chunk. The process can be described in the following steps:

1. `collect_particles_x`: Out of bound particles in the X direction are extracted from the chunk and placed in the correct target chunk queue for local exchange.
2. `exchange_particles_x`: Each chunk looks for particles in the neighbour chunks target queues and moves them to itself.

Usually only two target queues are required for each chunk, as the particles can only move one chunk per iteration. However, in the initial iteration after the initialization of the particle positions, they can move to any other chunk, and the process is subsequently more computationally expensive. We will only focus in the general case involving only the two neighbours, as the initialization iteration can be disregarded when comparing the time against the whole simulation.

Each step can be implemented using tasks with dependencies, in order to exploit local parallelism. One task collects the particles out of the chunk in the corresponding queues, so it needs to access only the current chunk.

```

for(i = 0; i < plasma->nchunks; i++)
{
    chunk = &plasma->chunks[i];
    /* Place each particle outside a chunk in the X dimension, in
       * the lout list */
    #pragma oss task inout(*chunk) label(collect_particles_x)
    for(is = 0; is < sim->nspecies; is++)
    {
        collect_particles_x(sim, chunk, is, global_exchange);
    }
}

```

The exchange process can now run in parallel, but the task can only run if the collecting process has finished in the neighbour chunks, as otherwise the queues are still being written. The dependencies can be placed in all involved chunks.

```

for (i = 0; i < plasma->nchunks; i++)
{
    chunk = &plasma->chunks[i];
    ...

    #pragma oss task inout(*chunk) \
        inout(*prev_chunk) inout(*next_chunk) \
        label(exchange_particles_x)
    {
        /* Only the two neighbours are needed */
        concat_particles(chunk, prev_chunk);
        concat_particles(chunk, next_chunk);
    }
}

```

Notice that in the first iteration the exchange step must wait for all the collecting tasks to finish, as the particles can be moved to any chunk, and thus we expect to see a slower iteration than the rest of the simulation. In the following steps, only the neighbours at  $i - 1$ ,  $i$  and  $i + 1$  are required to finish the exchange process.

However, there is a problem with the previous loop: as we create the dependencies with the next chunk before the next task is created, we are building a chain. Using `paraver` we can clearly see the chain in the trace graph, shown in the figure 10.1a, where no task can run in parallel until the previous one finishes. One solution to alleviate this problem is the use of colors, where the loops creates all tasks of the same color first, then the ones with the next color and so on. With three colors we ensure that the two tasks of the same color can run in parallel without concurrent access to the same chunk.

```

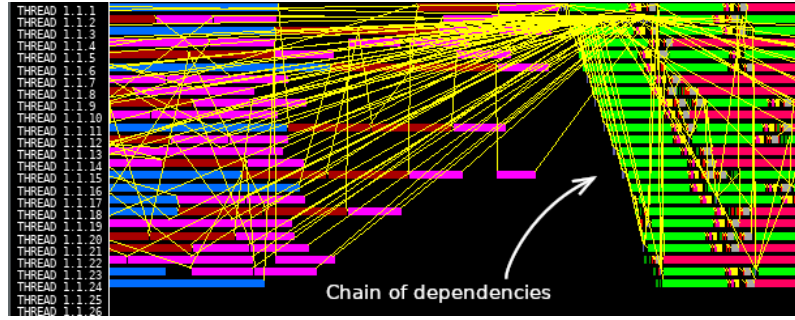
max_color = 3;

```

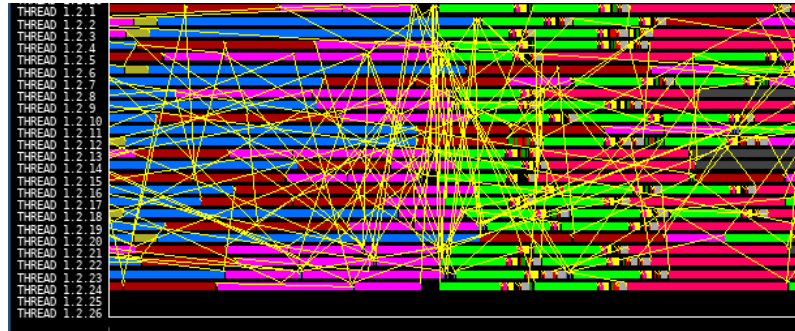
```

for(color = 0; color < max_color; color++)
{
    /* Use coloring to prevent a chain of dependencies */
    for(i = color; i < plasma->nchunks; i+=max_color)
    {

```



(a) Chain of dependencies observed



(b) The chain has been corrected

Figure 10.1: Comparison of two `paraver` traces using coloring tasks for communication.

```

chunk = &plasma->chunks[i];
...

#pragma oss task inout(*chunk) \
    inout(*prev_chunk) inout(*next_chunk) \
    label(collect_local_particles)
{
    /* Only the two neighbours are needed */
    concat_particles(chunk, prev_chunk);
    concat_particles(chunk, next_chunk);
}
}

```

In the figure 10.1b we can now observe how the chain has disappeared, and the holes are now fully covered by tasks running in parallel.

Once all exchange tasks are completed, all particles are now placed in the correct chunk in the X dimension, and only the Y movement is left.

### 10.1.2 Exchange in Y

Once the particles are placed in the correct chunk in the X dimension, the displacement to the correct chunk in the Y dimension involves sending the particles to another MPI process. The steps can be resumed as

1. `collect_particles_y`: Place each particle out of the chunk bounds in a queue

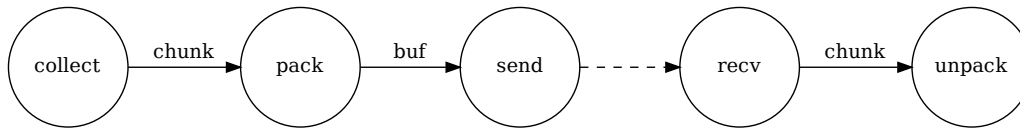


Figure 10.2: Graph of task and dependencies of particle communication in Y

(one for each target destination).

2. `pack_particles_y`: Pack the particles to be sent to the neighbour chunk in a message.
3. `send_particles_y`: Send the packed particles to each neighbour.
4. `recv_particles_y`: Receive the message with the packed particles.
5. `unpack_particles_y`: Unpack the particle message and place the particles in the chunk.

Similarly as for the horizontal direction, the particles exceeding the limits of each chunk in the Y dimension are placed in a queue. Once the particles are identified within a chunk, they are packed in a message in a contiguous memory region. This buffer is then sent using `MPI_Send` to the neighbour process.

The reception process works in the opposite order: each chunk receives the communication of the neighbour chunks in the vertical direction. Once a message is received is unpacked and the particles are added to the chunk. In the diagram 10.2 the dependencies of each step are shown in a graph.

Notice that all the MPI communication is independent of the neighbour chunks in the horizontal direction, and can be fully parallelized. Some constraints must be added to coordinate the vertical communications to guarantee that no simultaneous writes occur in the same chunk.

```

for(i = 0; i < plasma->nchunks; i++)
{
    chunk = &plasma->chunks[i];

    /* Collect particles in a queue that need to change chunk */
    #pragma oss task inout(*chunk) label(collect_particles_y)
    for(is = 0; is < sim->nspecies; is++)
    {
        collect_particles_y(sim, chunk, is, global_exchange);
    }

    /* Prepare the packet to be sent to the neighbour */
    #pragma oss task inout(*chunk) label(pack_particles_y)
    pack_particles_y(sim, chunk, i, global_exchange);
}
  
```

```
/* Finally send the packet */
#pragma omp taskwait label(send_particles_y_y)
send_particles_y(sim, chunk, i, global_exchange);

/* We cannot create here a task as we don't know the dependencies
 * when using MPI */
recv_particles_y(sim, chunk, global_exchange);
}
```



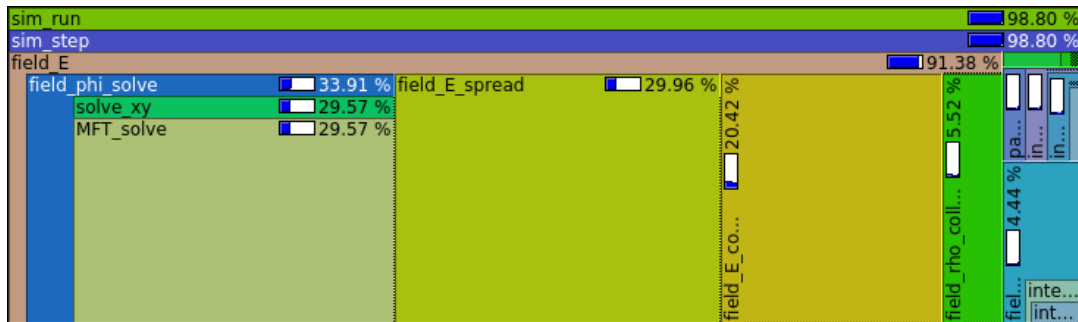


# Chapter 11

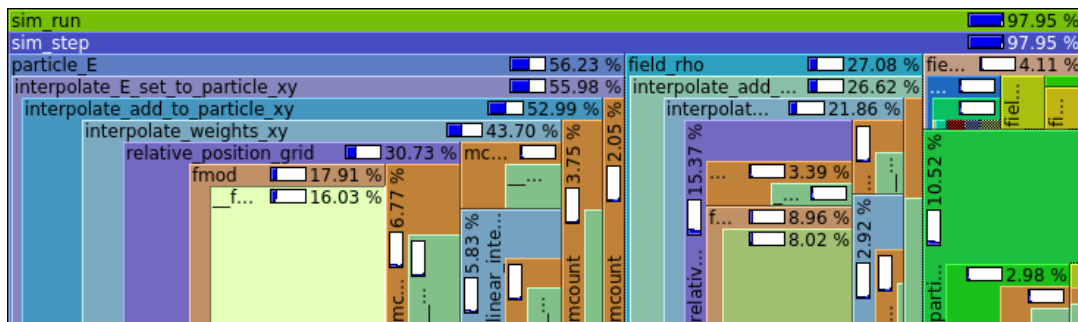
## Analysis

In order to reduce the amount of CPU time involved in each step of the simulation, the best strategy is to reduce the time spent in the most time consuming part.

The CPU time involved in each part of the simulation may depend on various factors, such as the number of grid points, the number of particles or the boundary conditions. As an example, consider a simulation with a large number of grid points, with few particles—the computation of the electric field (`field_E`) will dominate the simulation time, as shown in the figure 11.1a. In a case of a large number of particles and a smaller grid, the particle interpolation (`particle_E`) dominates the whole execution as seen in the figure 11.1b. In order to optimize the general use case,



(a) 1024 particles, 512x512 grid points



(b) 10240 particles, 64x64 grid points

Figure 11.1: Comparison of the time spent in each function at two different simulations.

different inputs will be tested and the main simulation steps will be characterized. Furthermore, different algorithms or methods may be used to improve the speed.

As an example, the LU algorithm is compared with the spectral method MFT.

## 11.1 Analysis with varying inputs

# Chapter 12

## Configuration



# Chapter 13

## Caveats and limitations

Here is a list of things that are not implemented in the simulator, but may be added in a future work.

- More than 2 dimensions
- Fully electromagnetic simulation
- Relativistic particle movement
- Heterogeneous architecture (GPU+CPU...)
- Energy conserving codes
- Visualization of big simulations (paraview)
- Replace simulation units, so we avoid factor multiplications
- Other interpolation methods (reduce noise at computational cost)

Caveats that need to be fixed

- Allow to specify plasma frequency
- Validation with other simulation codes



# Bibliography

- [1] F. F. CHEN, *Introduction to Plasma Physics and Controlled Fusion: Volume 1: Plasma Physics*, Plenum Press.
- [2] M. GALASSI, J. DAVIES, J. THEILER, B. GOUGH, G. JUNGMAN, P. ALKEN, M. BOOTH, AND F. ROSSI, *GNU Scientific Library Reference Manual*, Network Theory Ltd., third ed., 2009.
- [3] R. W. HOCKNEY AND J. W. EASTWOOD, *Computer Simulation Using Particles*, Taylor & Francis, Inc., Bristol, PA, USA, 1988.